Journal of Cardiovascular Disease Research
ISSN: 0975-3583,0976-2833 VOL 16, ISSUE 7, 2025

# The Use of NP-110, a RHAMM Peptide Mimetic, Reduces Capsular Fibrosis in a Novel Rodent Model of Radiation-Induced Capsular Contracture.

**1.Dr. P. Rajendra Kumar1; 2.Dr.Sasikanth Reddy; 3.Dr.Rubina Fathima**

1. Associate Professor, Department of General Surgery,Anjarkandy Medical College,Kannur,Kerala.
drrajendrapatwari@gmail.com
2. Assistant Professor, Department of General Surgery.
Sasisesi114@gmail.com
3. Junior resident, Department of General Surgery.

## Abstract

Capsular contracture is a common complication after breast implant surgery, worsened by radiation. This study tested NP-110, a RHAMM peptide mimetic, in a rat model with implants and radiation. NP-110 reduced fibrosis and collagen buildup, suggesting RHAMM may be a target to prevent capsular contracture.

## Introduction

Capsular contracture is a common, unpredictable complication after breast implant surgery, especially in patients with post-mastectomy or post-lumpectomy reconstruction and radiation. Up to 49.4% of these patients may experience significant contracture, and no non-surgical prevention methods currently exist.

## Definition and Pathogenesis of Capsular Contracture

Capsular contracture is a complication after breast implant surgery, graded by the Baker system (I–IV). Severe cases (grade IV) cause pain, deformity, and psychological distress, especially in patients who had radiation therapy. It results from an excessive fibrotic response to the implant, driven by chronic inflammation and myofibroblast activity. However, the exact molecular mechanisms remain unclear, limiting the development of effective treatments.

## Post Mastectomy Radiation Therapy

Post-mastectomy radiation therapy (PMRT) significantly increases the risk of capsular contracture in implant-based breast reconstruction, with rates up to 49.4%. Cosmetic outcomes are also worse in radiated patients. While two-stage reconstruction with tissue expanders aims to avoid radiation to the final implant, it does not significantly reduce contracture risk due to lasting radiation effects, including cell senescence and fibrosis. Some studies suggest higher failure rates when radiation targets expanders. Hypofractionated radiation (lower dose, shorter duration) shows promise in reducing short-term side effects (as seen in the FABREC trial), but long-term data is needed to confirm its impact on capsular contracture.

## Radiation Induced Fibrosis

As radiation therapy use increases, so does its impact on implant-based breast reconstruction. Radiation generates reactive oxygen species (ROS), leading to inflammation, tissue damage, and fibrosis. Key drivers include TGFB1, which promotes fibroblast-to-myofibroblast differentiation and collagen deposition via the Smad3 pathway. Radiation also upregulates Thy1, enhancing myofibroblast activity. These mechanisms contribute to dense capsule formation and capsular contracture. TGFB1, Smad3, and Thy1 are emerging as potential therapeutic targets to reduce radiation-induced fibrosis.

## Current Management of Capsular Contracture:

Capsular contracture remains a challenging complication with limited treatment options and high recurrence rates. Non-invasive methods like massage and ultrasound lack strong evidence. Closed capsulotomy is rarely used due to risks like implant rupture. The current gold standard is open surgery—capsulotomy or capsulectomy with implant exchange—but it carries risks such as pain, bleeding, and structural damage, especially in submuscular reconstructions. Despite surgery, recurrence rates can reach up to 54%, particularly in patients who had radiation therapy. Thus, treatment often prolongs recovery and may not guarantee resolution

## Therapeutic Targets of Interest

A number of therapeutic targets and potential pharmaceutical agents have been tested for the prevention and treatment of capsular contracture, as the scientific community searches for solutions to this pervasive complication.

### Anti-microbials

Bacterial biofilms may contribute to capsular contracture by causing chronic inflammation. Studies have shown a correlation between higher Baker grades and positive bacterial cultures from implants, especially with Staphylococcus epidermidis. Aseptic techniques and antiseptic irrigation during surgery may reduce risk, but biofilms aren’t found in all cases. There’s no clear evidence supporting post-op antibiotics, suggesting biofilms are one of several factors involved in contracture development.

### Anti-inflammatories

Anti-inflammatory agents like leukotriene receptor antagonists, cromolyn sodium, and corticosteroids show promise in reducing capsular contracture in animal models. Cromolyn sodium was the most effective, and montelukast reduced fibrosis in irradiated models. While these agents reduce inflammation and collagen production, there is limited clinical trial data, and systemic side effects may limit their use.

## Adipose Derived Stem Cells

Adipose-derived stem cells (ADSCs) have shown antifibrotic effects and may help reduce capsular contracture. Found in fat grafts, ADSCs improve skin quality post-radiation and reduce fibrosis markers like TGFB1 and collagen in animal studies. Clinically, fat grafting during or after implant surgery has led to sustained improvements in contracture, and in some cases, fat grafting alone resolved symptoms. As a minimally invasive option, it offers reduced risk and recovery time, though more clinical trials are needed to confirm its effectiveness.

## Acellular Dermal Matrix

Acellular dermal matrix (ADM) is increasingly used in breast reconstruction and is linked to reduced capsular contracture rates. ADM supports the implant and has been shown in studies to lower inflammation, fibrosis, and collagen deposition. Animal models confirm thinner, less fibrotic capsules with ADM use. Though the exact mechanism is unclear, it may act as a barrier to inflammation or disrupt capsule formation. Further research is needed to clarify how ADM prevents contracture.

## Hyaluronan

Hyaluronan (HA), a key extracellular matrix component, plays a role in inflammation and fibrosis depending on its molecular weight. Radiation-generated ROS can fragment HA into low molecular weight (LMW) forms, which trigger inflammation via receptors like CD44 and TLR4, promoting fibrosis. Studies show higher serum HA levels in patients with severe capsular contracture, suggesting a potential biomarker. However, HA appears reduced in capsule tissue itself, and the specific molecular weights involved are unclear. More research is needed to clarify HA’s role in capsular fibrosis.

## Receptor For Hyaluronan Medicated Motility (RHAMM)

RHAMM (HMMR) is a protein involved in wound healing, tissue remodeling, and fibrosis. Under tissue stress, it moves to the cell surface and, with CD44, binds HA fragments to activate pro-inflammatory pathways like RAS-ERK1/2. RHAMM is normally low in healthy tissue but increases after injury, promoting fibroblast activity. Its absence impairs wound healing. Since fibroblasts and myofibroblasts are abundant in capsular contracture, RHAMM may play a key role, though more research is needed to clarify its involvement.

## RHAMM Function Blocking Peptide Mimetics

RHAMM's interaction with low molecular weight HA((LMW-HA) contributes to inflammation and fibrosis, making it a promising therapeutic target. Peptide mimics like P-15 and NP-110 have been shown to block RHAMM-HA signaling, reducing fibroblast activity, TGFB1 expression, and collagen production in models of wound healing and fibrosis. NP-110, in particular, prevents RHAMM from binding LMW-HA, leading to decreased fibrosis in animal models, including radiation-injured mammary fat pads. These findings support RHAMM inhibition as a potential strategy to reduce fibrosis in capsular contracture.

## Objectives and Aims

Objective 1: Replicate the rodent model of radiation-induced implant capsular contracture with NP-110 peptide intervention.

- Aim 1: Perform standardized surgical placement of a silicone implant under the right 4th mammary fat pad.
- Aim 2: Administer a one-time, blinded injection of 100 µg NP-110 or control peptide to the same site, following protocols from Truong et al.
- Aim 3: Deliver a single 26 Gy radiation dose using DeLyzer et al.'s custom setup.

Objective 2: Assess the antifibrotic effect of NP-110 on irradiated implant capsules.

- Aim 1: Evaluate fibrosis clinically using Baker and Kumar grading.
- Aim 2: Analyze capsule histology with Masson's trichrome and Picrosirius red staining to assess collagen structure.
- Aim 3: Measure collagen content via hydroxyproline and total protein assays.
- Aim 4: Compare NP-110 outcomes to control peptide, radiation-only, and non-radiated groups using prior data from DeLyzer et al.

## Methods

**Ethical Approval**:
All experiments were approved under Animal Use Subcommittee Protocol #2022-126 and followed standard operating procedures.

**Model Overview:**

This study builds on the rat model developed by DeLyzer et al. (based on prior work from Truong et al.) for radiation-induced capsular contracture.

- Custom 2cc silicone implants (Mentor, J&J) were surgically placed under the right 4th mammary fat pad.
- A single 26Gy dose of targeted radiation was administered 4 weeks post-implantation using a custom 3D-printed "ratform."

- The model reliably induces capsular contracture, measurable via clinical grading, histology, and fibrosis biomarker assays.

**Sample Size Calculation:**

Using power = 0.8, α = 0.05, and contracture prevalence of 100% (radiated) vs 20% (control):

- Calculated minimum sample size per group = 6 animals
- With 10% attrition allowance, final group size = 7 animals
- DeLyzer et al. previously showed statistically significant results using this sample size.

## Current Experimental Overview

Experiments were conducted on 14 retired female Sprague Dawley breeder rats (Charles River, typical age 6–12 months), housed in pairs under controlled conditions with standard diet, water, and enrichment.

- Implant surgery was performed first.
- Four weeks later, all animals received 26Gy targeted radiation to the implant site.
- During radiation (under anesthesia), rats were injected with 100 µg of either the active NP-110 peptide or a scrambled control peptide, targeted to the right 4th mammary fat pad.
- Injections were performed blinded, and researchers remained blinded throughout the study and analysis.
- Endpoint: Four weeks post-radiation, allowing for measurable clinical and histological capsule formation (based on previous model data).
- Rats were monitored weekly for health, weight, and met pre-defined removal criteria if needed.

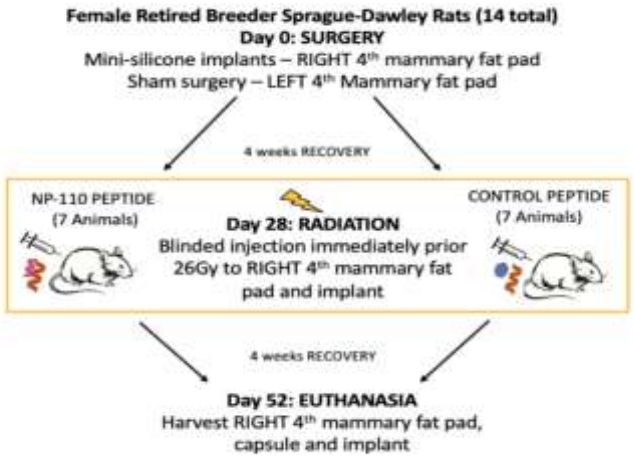


**Figure 1.** Overview of timeline for animal experiments. All animals undergo surgery at day 0, recover for 4 weeks and then are injected with either active peptide NP-110 or scrambled control peptide to the 4th mammary fat pad prior to radiation with 26Gy.

## Surgery Protocol

Surgeries were performed at LRCP VRL under isoflurane anesthesia.

- Anesthesia: Induced in a chamber, then maintained via nose cone on a warmed operating table.
- Pre-op Care: Rats received a single subcutaneous dose of meloxicam (1–2 mg/kg). Eyes were lubricated, and body temperature monitored.
- Site Preparation: Hair around the 4th mammary fat pad (2 cm diameter) was clipped and disinfected with chlorhexidine, alcohol, and betadine (repeated twice).
- Surgical Procedure:
    - A small incision was made below the 4th mammary fat pad on both sides.
    - A pocket was dissected under the right fat pad, and a 2cc custom silicone implant (Mentor, 2 cm diameter × 1 cm height) was inserted after betadine irrigation.
    - The left side underwent sham surgery (dissection only, no implant).
- Closure & Recovery: Incisions were closed using absorbable 5-0 vicryl sutures and skin glue. Animals were recovered under oxygen and returned to their cages once fully awake.

21

**Figure 3.** "Mini" cohesive silicone gel implants supplied by Mentor/J&J. Base diameter is 2cm, and projection of the implants is 1cm.

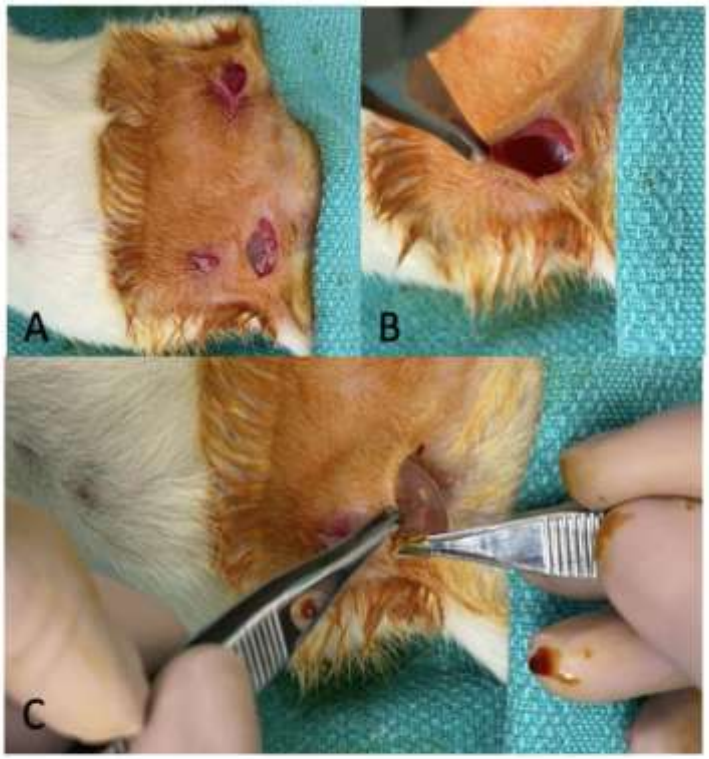


**Figure 2.** Incisions made under the right and left 4th fat pads (A) with demonstration of the sub glandular pocket that was developed (B) and insertion of the implant into the implant pocket after irrigation with betadine solution (C).

## Post-Operative Monitoring

Animals were monitored daily for the first 7 days post-operatively and then weekly thereafter. Weight was recorded along with recording body condition score and a standardized scoring template for behavior, appearance, activity, and dehydration and pain. The surgical site was also examined and assessed site for complications. The implant was examined weekly for evidence of capsular contracture and given Baker grading score using the criteria described in Table 1 below. In our study we scored Baker grade from 1-3 as a

**Table 1:** Baker grading score for implant capsular contracture[4].

| Baker Grade | Description |
|---|---|
| I | Soft, mobile implant |
| II | Implant is palpable but not visible |
| III | Implant is easily palpable, and visible |
| IV | Implant is hard, distorted, and painful |

grade 4 contracture requires pain to be present, and could therefore not be accurately assessed in our model.

## Peptide Preparation and Delivery Protocol

The NP-110 active peptide (sequence: Ac-KLKDENSQLKSEVSK-$NH_2$) and a scrambled control peptide (NP-0111) containing the same amino acids in a different sequence were prepared by the Luyt lab and verified via mass spectrometry. Peptides were stored at –80 °C and reconstituted in Hank's Solution to a concentration of 1 µg/µL under sterile conditions. To maintain blinding, vials were labeled A and B by an individual not involved in the study, and all personnel remained blinded until data analysis was complete. During the radiation

**Figure 4.** Injection of peptide solution into the right 4th mammary fat pad of 100uL, for a 100ug dose, directly under the right 4th nipple taking care to not violate the implant capsule.

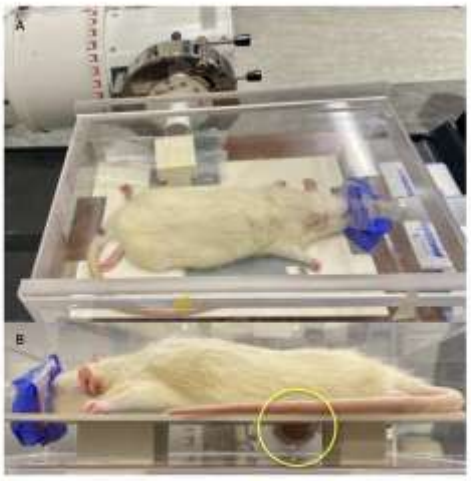


**Figure 5.** Positioning of a rodent on the 3D printed "Rat-form" showing the targeting of the Orthovoltage unit 3cm cone centered at the implant and fat-pad which lies below the rest of the rats body highlighted by the yellow circle (B).

procedure, animals under isoflurane anesthesia received a subcutaneous injection of 100 µL (100 µg) of peptide into the right 4th mammary fat pad, carefully avoiding the implant pocket by lifting the nipple and injecting with a 30G needle. Odd-numbered animals received peptide A, and even-numbered animals received peptide B.

## Radiation Protocol

Radiation was administered under the supervision of Dr. Eugene Wong at the London Regional Cancer Centre using a clinically active orthovoltage unit. A total of 26 Gy was delivered in a single session—13 Gy from each lateral side—targeted specifically to the right 4th mammary fat pad and underlying implant. The left side (sham surgery) received no radiation. Following peptide injection, animals were placed prone on a custom 3D-printed "Rat-form" that exposed only the implant region to the radiation field, while the rest of the body was shielded with lead. A 3 cm cone was attached to the orthovoltage machine and positioned in contact with the radiation cage to ensure precise targeting. Beam accuracy was verified in some animals using test film that darkened upon exposure. Each side received 3360 MU (equivalent to 13 Gy), for a total dose of 26 Gy over approximately 24 minutes. The 4–6 cm penetration of the orthovoltage beam ensured full coverage of the 2 cm implant. Animals were continuously monitored via video for breathing and movement and were recovered in individual cages following radiation and temperature assessment.

## Post-Radiation Monitoring

Animals were monitored daily for the first 7 days post-radiation and then bi-weekly thereafter. Weight was recorded along with recording body condition score and a standardized scoring template for behavior, appearance, activity, and dehydration and pain.

**Table 2.** Kumar Score for radiation skin damage[60].

| Kumar Score | Skin Changes |
|---|---|
| 1 | No effect |
| 1.5 | Minimal erythema, mild dry skin |
| 2 | Moderate erythema, dry skin |
| 2.5 | Marked erythema, dry desquamation |
| 3 | Dry desquamation, minimal dry crusting |
| 3.5 | Dry desquamation, dry crusting, superficial minimal scabbing |
| 4 | Patchy moist desquamation, moderate scabbing |
| 4.5 | Confluent moist desquamation, ulcers, large deep scabs |
| 5 | Open wound, full thickness skin loss |
| 5.5 | Necrosis |

The surgical site was also examined and assessed site for complications. The implant continued to be examined bi-weekly and scored using the Baker grade scale (Table 1). The animals abdomen was also examined and scored using the Kumar Score for radiation skin changes seen in Table 2.

## Tissue Collection

At four weeks post-radiation, animals were euthanized via isoflurane overdose in accordance with SOP protocols. Final weight, a photograph of the surgical area, and Baker score were recorded. The right 4th mammary fat pad, along with the implant and capsule, was carefully dissected en bloc using a #15 blade to preserve tissue architecture. The left 4th mammary fat pad (sham side) was also harvested for potential future studies. All tissues were immediately fixed in 10% neutral buffered formalin (NBF). Tissue processing was performed by histologist Carl Potenska, where samples underwent serial dehydration and were embedded in paraffin wax with the implant in situ. After sectioning, implants were removed, the cavities were filled with paraffin, and blocks were reheated and cooled twice to maintain capsule structure. Sections were cut at 10 µm thickness and mounted on slides. Only the right (implant side) tissues were used for histological staining and analysis, as the focus of this study was on radiation-induced capsular changes.

## Hematoxylin and Eosin

Tissue sections were stained with Hematoxylin and Eosin (H&E). Sections from all animals in the study were included. Two slides per animal were stained, one superficial and one deeper section. Image acquisition was conducted using an Aperio ImageScope,(Leica

Microsystems, Buffalo Grove, Il, USA) and associated software was used tocapture images of each slide. One image of the entire slide, and a representative image of the capsule at 10X magnification were taken.

## Masson's Trichrome

Tissue sections from the right (implant) side were stained for collagen using Masson's Trichrome, which stains collagen fibers blue. Five sections at varying depths were stained per animal. Images were captured using the AperioImageScope system, including whole-slide scans and four randomly selected 10X magnified fields containing intact capsular tissue and adjacent fat pad. Damaged or unfocused areas were excluded. Image analysis was performed in ImageJ using the Masson's Trichrome deconvolution function to isolate blue pixels representing collagen. The polygon tool was used to define capsular regions, and both the area and mean grey value (indicating stain intensity) were measured. An average of 20 regions of interest (ROIs) per animal was calculated, with higher grey values indicating greater collagen content.

## Picrosirius Red

Tissue sections were stained using the Picrosirius Red Staining Kit to evaluate collagen bundling, with five sections per animal from the implant (right) side stained at varying depths. Slides were examined under polarized light using Abrio 2.2 software, and four 40X magnified regions of interest (ROIs) focusing on the capsule and adjacent fat pad were captured per slide by a blinded assessor. In polarized light, collagen fibers display birefringence where color shifts from blue to red indicate increasing fiber thickness, with red reflecting dense collagen typical of fibrosis. Image analysis was performed using ImageJ: images were split using the RGB stack function, and the red channel was selected. A threshold of 220–255 was applied to isolate red pixels, and the polygon tool was used to define the capsular tissue area. The percentage of red-stained area was calculated and averaged across 20 ROIs per animal to quantify collagen bundling.

## Immunohistochemistry

Immunohistochemistry staining for TGFB1 and alpha-smooth muscle actin (aSMA) was conducted using a 3-day protocol on 42 slides (three per animal). On Day 1, slides were deparaffinized with two 15-minute xylene washes, followed by sequential washes in 100%, 95%, and 70% ethanol, and rehydrated in distilled water and 1x TBS. Antigen retrieval was performed in 10 mM sodium citrate buffer (pH 6.0) using a microwave protocol. After cooling, slides were blocked with 3% BSA for 1 hour, encircled with wax, and incubated overnight at 4°C with 50 µL of primary antibody (TGFB1: Abcam ab215715; aSMA: Abcam ab124964), each diluted 1:100 in TBS. On Day 2, slides were washed, re-waxed, and incubated for 2 hours at room temperature with Alexa Fluor™ 488-conjugated goat anti-rabbit IgG secondary antibody (Thermo-Fisher A-11034), also diluted 1:100. After washing, slides were mounted with ProLong™ Gold Antifade Mountant containing DAPI. On Day 3, stained slides were imaged using an Olympus Fluoview microscope and associated software.

## Biochemical Assays

The second method for quantifying fibrosis in tissue samples involved hydrolysis-based assays to measure hydroxyproline (a collagen biomarker) and total protein content. Hydroxyproline levels (Abcam Cat # ab222941) were used to estimate collagen deposition and fibrosis severity, normalized against total protein (Quickzyme Cat # QZBtotprot1) to correct for tissue variability. Twenty-five 10 µm sections from the right 4th implant capsule and mammary fat pad per animal were hydrolyzed in 6N HCl at 95°C for 16 hours. After centrifugation at 13,000 rpm to separate paraffin, the supernatant was serially diluted, with a 1:16 dilution chosen for both assays based on pilot testing against the standard curve. Assays were run in 96-well plates with six technical replicates per sample, and absorbance was measured at 570 nm (total protein) and 560 nm (hydroxyproline) using a Biotek Synergy HTX plate reader. Concentrations were calculated from standard curves, and average values per animal were used to compute the hydroxyproline-to-total protein ratio, with higher ratios indicating greater fibrosis.

# Results

## Qualitative Outcomes

Fourteen retired female Sprague-Dawley rats (average weight 332g, range 285–390g) were included in the study, with all undergoing surgery and radiation without major complications. One animal (Animal 9) presented with a soft, mobile mass in the right upper limb, but veterinary assessment allowed it to remain in the study as the mass was distant from the operative site and did not impair function. One intra-procedural complication occurred during radiation of Animal 3 (NP-110 group), which received only a partial dose due to anesthetic equipment failure; its data was excluded from analysis. All animals initially had Baker grade 1 contractures post-surgery and remained so one week post-radiation. By week four, all animals showed increased contracture severity. Notably, all control peptide animals progressed to Baker grade 3, whereas two animals in the NP-110 group had only Baker grade 2 contractures, suggesting a potential protective effect of NP-110. Additionally, NP-110 treated animals had lower average Kumar scores for skin toxicity, although this was not statistically significant. Dissections revealed more adherent capsules in control animals, correlating with higher fibrosis. Sham surgery sites on the contralateral side healed without significant complications, confirming the localized nature of radiation-induced effects.

# Discussion and Conclusion

The primary objective of this thesis was to investigate the role of the RHAMM pathway in the development of radiation-induced capsular contracture using a novel rodent model previously developed by T. DeLyzer et al. This was achieved through administration of NP-110, a RHAMM function-blocking peptide mimetic, in order to assess its effect on capsule fibrosis. The involvement of RHAMM in capsular contracture had not been previously studied, and this work aimed to address that gap. Clinical assessments revealed that animals treated with NP-110 had lower scores for radiation-induced skin changes and capsular contracture severity. Histologically, the NP-110 group demonstrated significantly reduced collagen deposition and less-dense collagen bundling compared to controls, as shown by Masson’s trichrome and Picrosirius red staining. However, hydroxyproline assays did not show a statistically significant difference in collagen content between groups. Overall, these

findings suggest that RHAMM signaling contributes to the development of capsular fibrosis, and that targeting this pathway with NP-110 may offer a promising non-surgical approach to mitigate or prevent capsular contracture following implant-based breast reconstruction.

## Objective 1 Discussion

We successfully replicated the previously established rodent model for radiation-induced implant capsular contracture developed by T. DeLyzer et al., incorporating the additional intervention of NP-110 or scrambled control peptide injection. Despite being led by a junior surgical trainee (K. Minkhorst), the model was straightforward to reproduce, with surgical times remaining efficient—approximately 15–20 minutes per animal, with total induction to recovery times between 35–45 minutes. The procedure was completed in two morning sessions with assistance from T. DeLyzer and N. Lewandoski, highlighting the practicality and feasibility of the model for future research. The peptide injection protocol was modified from the original Truong et al. study by administering the 100 μg dose immediately prior to radiation rather than post-radiation day 1, reducing anesthetic exposure and procedural burden while still achieving effective results. Landmark-based subcutaneous injection at the 4th right nipple replaced ultrasound-guided delivery, simplifying the protocol and increasing its accessibility without compromising outcomes. A clinically active Orthovoltage unit was used to administer 26 Gy of radiation in a single session, a slight deviation from DeLyzer's original protocol due to equipment changes, but still effective in inducing measurable fibrosis. The timing—radiation at 4 weeks post-implant and study endpoint at 4 weeks post-radiation—was maintained as per the original model, aligning with both prior experimental data and clinical timelines of capsular contracture development. Overall, the modifications made improved the model's accessibility while preserving its ability to reproduce clinically relevant capsular fibrosis, demonstrating the RHAMM pathway's role and the therapeutic potential of NP-110.

## Conclusions and Limitations of Objective 1

The primary aim of Objective 1 in this thesis was to replicate the established model of radiation-induced implant capsular contracture developed by DeLyzer et al., with the addition of an experimental therapeutic agent. The success in replicating this model reinforces its validity and robustness as a platform for studying capsular contracture. Although there was a two-year gap since the original work, the main operator (K. Minkhorst), a junior surgical trainee who previously assisted in the initial study, was able to independently and efficiently perform the procedure—demonstrating the model's straightforward and replicable nature. A key strength of the model is its anatomical relevance; by placing implants in the mammary fat pad rather than the dorsal region, the model better simulates the clinical environment of breast implants. While it lacks certain clinical features—such as post-mastectomy tissue trauma and subpectoral implant placement with acellular dermal matrices—it still offers advantages over dorsal models, which often lack mammary-specific structures like the nipple. These limitations are recognized as necessary compromises, as sub-muscular placement in the abdomen would risk intra-peritoneal positioning. Therefore, the mammary fat pad model serves as a valuable addition to the repertoire of available animal models, especially for studying the microenvironment of implant-associated fibrosis. A further limitation was the use of a different radiation source—an orthovoltage unit instead of the previously used linear accelerator. While orthovoltage radiation has reduced tissue penetration, it proved effective in this context due to the superficial location of the fat pad and implant. The observed radiation-

induced skin changes and fibrosis confirm that the 26 Gy dose delivered via orthovoltage was sufficient to induce contracture. This also suggests that the model remains applicable across different institutional setups, supporting broader adoption and reproducibility in future research.

## Objective 2 Discussion

The objective of evaluating the effect of NP-110 on radiation-induced capsule fibrosis demonstrated that local administration of this RHAMM-inhibiting peptide significantly reduced fibrosis and collagen bundling compared to a scrambled control peptide, radiation alone, and even matched levels seen in non-radiated controls. Clinically, all animals developed at least grade 2 capsular contracture post-radiation, with the control peptide group progressing to grade 3, while two animals in the NP-110 group maintained less severe grade 2 contractures. Histological analyses using Masson's Trichrome and Picrosirius Red confirmed that NP-110-treated capsules had significantly reduced collagen deposition and less dense bundling, key features associated with less fibrotic and more pliable tissues. Notably, the Masson's Trichrome results revealed no significant difference between NP-110-treated capsules and non-radiated controls, reinforcing the efficacy of NP-110 in mitigating radiation-induced fibrosis.Re-analysis of previous data using improved, consistent image capture and ROI selection methods further validated these findings, showing reproducible outcomes that strengthen the model's credibility. Immunofluorescent staining for TGF-β1 and αSMA—both markers associated with fibrosis and myofibroblast activity—trended lower in NP-110-treated tissues but did not reach statistical significance, likely due to sample size limitations, timing of tissue harvest post-radiation, and spatial heterogeneity of marker expression. Since TGF-β1 peaks early after radiation exposure, measuring at four weeks may have missed the window of peak expression, limiting interpretability of these markers in the current study.Hydroxyproline assays, used as a biochemical correlate of collagen content, did not show significant differences between groups. This contrasted with earlier findings and may be attributed to assay changes by the manufacturer, technical limitations from inconsistent tissue sectioning, and variability in fat pad inclusion. This highlights the need for refined biochemical techniques or alternative quantitative collagen assessments in future studies.Overall, the findings strongly support the antifibrotic potential of NP-110 in preventing radiation-induced capsular contracture. The peptide's effect on both collagen quantity and organization suggests that RHAMM signaling plays a central role in fibrotic remodeling, likely through downstream interactions with TGF-β1 and myofibroblast activation. While some biochemical and immunohistochemical findings did not achieve statistical significance, likely due to technical and sample size constraints, the consistent histological and qualitative data provide compelling evidence for further exploration of RHAMM-targeted therapies as a non-surgical option to prevent or mitigate capsular contracture following implant-based breast reconstruction.

## Conclusions and Limitations of Objective 2

In conclusion, this study provides compelling evidence that NP-110, a RHAMM function-blocking peptide, significantly reduces radiation-induced capsular fibrosis, highlighting the

RHAMM signaling pathway as a promising therapeutic target in the prevention of capsular contracture. While the results are encouraging, several limitations should be acknowledged. Notably, the absence of mRNA or protein-level analyses due to the chosen tissue preservation methods restricted molecular insight into the mechanistic effects of NP-110. Although hydroxyproline assays were utilized as an alternative biochemical marker, high variability and lack of significant findings in this assay suggest that greater technical replication and improved tissue sampling strategies are warranted in future studies. Additionally, the one-time dose of 100 μg NP-110, though effective, was not tested against multiple doses or time points, nor was its post-radiation stability assessed—raising questions about optimal dosing regimens and peptide durability under radiation exposure. Future work should explore longitudinal dosing, tissue-level NP-110 quantification, and transcriptomic profiling at various post-radiation time points to better characterize the therapeutic potential and mechanism of RHAMM inhibition. Despite these limitations, the successful replication of the animal model and the consistent histological improvements observed in NP-110-treated animals underscore the potential for RHAMM-targeted therapies to mitigate implant-related fibrosis in clinical settings.

## Significance and Future Directions

To our knowledge, this study is the first to evaluate the effect of NP-110, a RHAMM function-blocking peptide, on implant capsule fibrosis using a novel rodent model of radiation-induced capsular contracture. Building upon previous work from the Turley lab demonstrating NP-110's antifibrotic effects in irradiated mammary fat pads, our findings provide further evidence that the RHAMM signaling pathway is involved in the development of capsule fibrosis. Given that the pathogenesis of capsular contracture—particularly in post-mastectomy, irradiated patients—remains poorly understood, this study highlights RHAMM as a novel target for therapeutic intervention. Current literature has focused on broad-acting fibrotic regulators like TGFB1 and SMAD pathways, which may be suboptimal due to their systemic roles. In contrast, RHAMM represents a more specific and potentially safer target. Importantly, our results show that local NP-110 injection via surface landmarking is feasible and effective, suggesting a clinically translatable approach. However, concerns regarding the practicality of repeated local injections—such as patient discomfort, sterility, and potential implant compromise—warrant investigation into alternative delivery routes. Moreover, since RHAMM blockade has also been shown to enhance adipogenesis in irradiated tissue, future studies could explore combination therapies with autologous fat grafting. This may improve fat graft survival and further reduce fibrosis, offering a dual benefit in breast reconstruction patients. Overall, our work supports RHAMM inhibition as a promising non-surgical strategy for mitigating radiation-induced capsular contracture.

## Conclusion

The investigation presented in this thesis has provided valuable insight into the role of RHAMM in the pathogenesis of radiation-induced capsular contracture and has laid the foundation for the development of potential non-surgical therapeutic strategies to mitigate this common and challenging complication of implant-based breast reconstruction. By replicating and modifying an established rodent model and evaluating the effects of the RHAMM function-blocking peptide NP-110, this study has generated several key findings.

First, the successful replication of the rodent model confirms its feasibility and reproducibility, even when conducted by a junior surgical trainee. Minor modifications to the protocol—such as the use of a clinically active Orthovoltage radiation unit—did not compromise the model's ability to induce significant radiation-associated fibrosis, supporting the robustness and adaptability of the model for future studies. Additionally, the timing and method of peptide delivery were optimized for practicality and safety, demonstrating an accessible approach for preclinical testing.

Second, NP-110 treatment showed promising anti-fibrotic effects. Qualitatively, animals receiving NP-110 demonstrated reduced implant capsule fibrosis and radiation-induced skin changes compared to those receiving a control peptide. Quantitative histological analyses using Masson's trichrome and Picrosirius red staining further confirmed these findings, showing significantly decreased collagen deposition and bundling in the NP-110 group. Notably, the capsule morphology in NP-110 treated animals was comparable to that seen in non-radiated controls, suggesting that NP-110 effectively prevents the development of fibrosis.

Despite these encouraging findings, several limitations warrant consideration. The absence of mRNA expression profiling and the variability in hydroxyproline assay results highlight the need for additional studies to better characterize the molecular mechanisms of NP-110. Future work should include transcriptomic analyses and explore alternative collagen quantification methods. Moreover, testing different doses, delivery timings, and repeat administration regimens of NP-110 could help refine its clinical application.

In summary, this thesis adds to the growing body of evidence supporting the involvement of RHAMM in fibrosis and identifies RHAMM inhibition via NP-110 as a promising therapeutic approach to prevent radiation-induced capsular contracture. While further validation is needed, these findings represent a meaningful advancement in the pursuit of effective, non-surgical interventions to improve outcomes for patients undergoing implant-based breast reconstruction. With continued research, the goal of reducing the incidence and burden of capsular contracture may be within reach.